

Experimental Vacuum Squeezing in Rubidium Vapor via Self-Rotation

J. Ries, B. Brezger, and A. I. Lvovsky

*Fachbereich Physik, Universität Konstanz, D-78457 Konstanz, Germany**

(Dated: July 23, 2018)

We report the generation of optical squeezed vacuum states by means of polarization self-rotation in rubidium vapor following a proposal by Matsko *et al.* [Phys. Rev. A **66**, 043815 (2002)]. The experimental setup, involving in essence just a diode laser and a heated rubidium gas cell, is simple and easily scalable. A squeezing of (0.85 ± 0.05) dB was achieved.

PACS numbers: 42.50.Lc, 42.50.Dv, 42.50.Nn

a. Introduction Squeezed states of a radiation field are nonclassical states whose field-quadrature noise is phase dependent with a minimum below the shot noise level. First investigated theoretically [1] and generated experimentally [2, 3] in the 1980's, these states awoke initial interest as a way of overcoming the shot-noise precision restrictions in optical measurements [4, 5] and enhancing the capacity of communication channels [6]. Further interest to squeezed light was triggered by recent advances in the field of quantum information and communication. In this context they are viewed primarily as a means of generating quadrature entanglement [7], a valuable resource that can be applied, for example, for quantum teleportation [8], computation [9], cryptography [10] and manipulation of atomic quantum states [11]. Protocols of error correction [12, 13] and entanglement purification [14] have been elaborated, establishing continuous variable entanglement as one of the most promising tools for quantum information technology.

A number of techniques for producing squeezed states of light have been developed, using for instance four wave mixing in atomic vapor [15], Kerr effect in cold atoms [16] or optical fibers [17, 18], optical parametric amplifiers [3]. All these methods require rather complicated setups that cannot be scaled easily, effectively preventing their practical application for the quantum information purposes. In the present paper we demonstrate a simple, scalable squeezed vacuum source which consists in essence of a continuous-wave (cw) diode laser and an atomic rubidium vapor cell. Easy and inexpensive generation of multiple Einstein-Podolsky-Rosen-entangled modes lies at hand, making them available to a variety of experiments and applications.

We make use of a phenomenon known as cross-phase modulation squeezing [19]: if linearly polarized light propagates through a nonlinear medium in which elliptical light would undergo polarization self-rotation, the orthogonal vacuum mode gets squeezed. Self-rotation and the associated squeezing effect are present in any Kerr medium but are especially strong in atomic vapor due to its large optical nonlinearity near resonance. To achieve squeezing it is sufficient to use a moderately intense cw

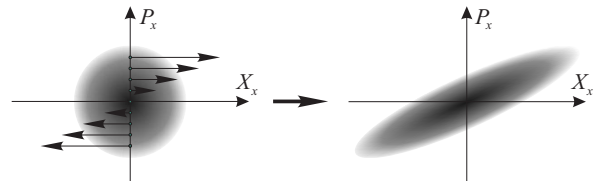


FIG. 1: Transformation of the phase space: a Wigner function describing the state of the probe field in the mode polarized orthogonally to the strong pump beam. Self-rotation results in a linear shear of phase space (Eqs. 3 and 4). The circular phase-space quasiprobability density describing the vacuum state is transformed into squeezed vacuum.

diode laser as a pump. Pulsed lasers or cavities are not needed and the diode laser does not even have to be frequency stabilized.

b. Theory The theory of squeezing via polarization self-rotation for the single mode case has been given in Ref. [20]. Here we present its brief quasiclassical overview. A detailed multimode description including the degrading effects of resonance fluorescence, phase mismatch and absorption will be published elsewhere.

Interaction with an elliptically polarized light field can cause an initially isotropic $\chi^{(3)}$ -nonlinear medium to become circularly birefringent: the two circular components of different intensities propagate with different phase velocities. Specifically in atomic vapor, the mechanisms leading to this birefringence include optical pumping, ac Stark shifts, as well as ac Stark shift induced quantum beats and Bennett structures [21]. Propagating through a cell of length l , the polarization ellipse of light will rotate by an angle φ which is proportional to the ellipticity $\epsilon \ll 1$:

$$\varphi = gl\epsilon, \quad (1)$$

with the self-rotation parameter g dependent on the incident light intensity and frequency.

Consider a monochromatic, elliptically polarized light field of frequency ω propagating in the z -direction. The complex field amplitudes in the two linear polarization components are given by \mathcal{E}_x and \mathcal{E}_y , with $|\mathcal{E}_x| \ll |\mathcal{E}_y|$. Assuming the “pump” amplitude \mathcal{E}_y real, we decompose the “probe” x -field into two real quadrature components in and out of phase with the pump field:

*URL: <http://www.uni-konstanz.de/quantum-optics/quantech/>

$\mathcal{E}_x(z) = X_x(z) + iP_x(z)$. Then the ellipticity ϵ of the laser light is given by

$$\epsilon \approx \frac{P_x(z)}{\mathcal{E}_y(z)}. \quad (2)$$

The resulting self-rotation by $\varphi \ll 1$ causes the pump field to contribute its fraction $\varphi\mathcal{E}_y$ into the x -polarization, namely into the X_x quadrature which is in phase with \mathcal{E}_y :

$$X_x(l) = X_x(0) + \varphi\mathcal{E}_y = X_x(0) + glP_x(0) \quad (3)$$

$$P_x(l) = P_x(0), \quad (4)$$

\mathcal{E}_y and ϵ remain effectively unchanged.

We now assume the x -polarized light field as classical noise described by a probability distribution in the quadrature plane (Fig. 1). To describe slow fluctuations, we regard the propagation of a light field described by $X_x(z)$, $P_x(z)$ and \mathcal{E}_y through the medium under stationary conditions. A random quadrature component $P_x(0)$ results in a small random ellipticity according to Eq. (2). The propagation through the cell will displace the point (X_x, P_x) in the phase space as described in Eqs. (3) and (4). The phase space probability distribution experiences a linear shear, resulting in reduction of the noise in some phase quadratures below the original level.

Although the above treatment is purely classical, it is completely identical in application to the quantum quadrature noise. Considering the Heisenberg evolution of the field-quadrature operators $\hat{X}_x(z)$ and $\hat{P}_x(z)$ we notice that the evolution described by Eqs. (3) and (4) can be associated with the interaction Hamiltonian $\hat{H} = \hbar gc \hat{P}_x^2 / 2$, c being the speed of light in the medium. Under a second order Hamiltonian, each point of the Wigner function — the quantum-mechanical analogue of the phase-space probability distribution — evolves according to the classical equations of motion [22]. The incoming symmetric Gaussian Wigner function of the vacuum is therefore transformed into an elliptical Wigner function of a minimum uncertainty squeezed vacuum state.

In a homodyne measurement such a state results in a quadrature noise depending on the local oscillator phase χ (cf. [20]):

$$\begin{aligned} \langle \Delta E_x(\chi, l)^2 \rangle & \quad (5) \\ &= \frac{\mathcal{E}_0^2}{4} ((1 - al)(1 - 2gl \sin \chi \cos \chi + g^2 l^2 \cos^2 \chi) + al). \end{aligned}$$

Here $\frac{\mathcal{E}_0^2}{4}$ is the standard quantum noise limit (SQL) associated with the vacuum state, and we have taken into account absorption of a small fraction $al \ll 1$ of the squeezed light after passing the medium. This treatment of absorption is approximate because some of the light energy is actually lost in the atomic vapor along the propagation path. However, it permits to account for one essential feature of our experimental result: the minimum uncertainty property is lost when $gl > 0$ and $al > 0$.

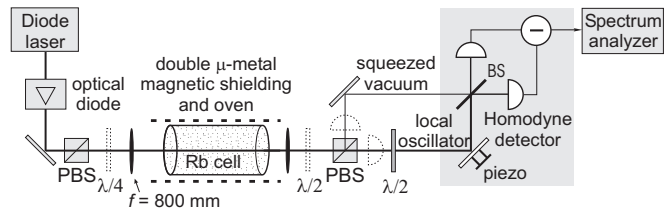


FIG. 2: Experimental setup. The second polarizing beam splitter (PBS) separates the x -polarized pump beam containing the squeezed vacuum from the y -polarized pump beam. The $\lambda/2$ plate rotates the polarization of the pump which is then used as the local oscillator in balanced homodyne detection, the piezoelectric transducer scans its phase. Dashed contours show optical elements used in the self-rotation measurement and/or the mode-matching alignment (see text).

c. Experimental apparatus The scheme of our experimental setup is shown in Fig. 2. A free running external cavity diode laser (Toptica DL-100) delivered 35 mW of optical power in a single mode at a wavelength of 780 nm, tunable across the rubidium $D2$ line. The beam was shaped with a pair of cylindrical lenses and a polarizing beam splitter (PBS) purified the linear polarization. The beam was focused by a lens ($f = 800$ mm) into a heated and magnetically shielded 75 mm rubidium cell which had optical quality anti-reflection coated windows and was filled with the nearly pure isotope ^{87}Rb . With a focal beam diameter of $600 \mu\text{m}$ we operated in a high saturation regime.

To determine the polarization self-rotation parameter gl a fine-adjustable $\lambda/4$ plate was placed in front of the cell. Its rotation angle in radians was equal to the generated ellipticity ϵ . The outputs of the second PBS were directly fed into two photodiodes. A $\lambda/2$ plate placed after the cell was adjusted so that the DC photodiode signals S_1 and S_2 were exactly equal when the laser was detuned far from the resonance. This “balanced polarimeter” was sensitive to the polarization ellipse rotation while being insensitive to changes in ellipticity. The rotation angle $\varphi \ll 1$ can be determined from the photodiode signal difference [21]:

$$\varphi = \frac{S_1 - S_2}{2(S_1 + S_2)} \quad (6)$$

By recording S_1 and S_2 while scanning over the rubidium $D2$ line for many different initial small ellipticities $\epsilon \ll 1$, the self-rotation parameter gl for each laser detuning was determined by polynomial fitting. Fig. 3 shows gl and the absorption coefficient al for our working temperature of 70°C . Note that a relatively high transmission on resonance is due to very high saturation of the atomic transition — in the linear small signal regime, the rubidium vapor is optically dense.

To measure the quantum field quadrature noise we employed the standard balanced homodyne detection technique. The y -polarized component of the laser beam

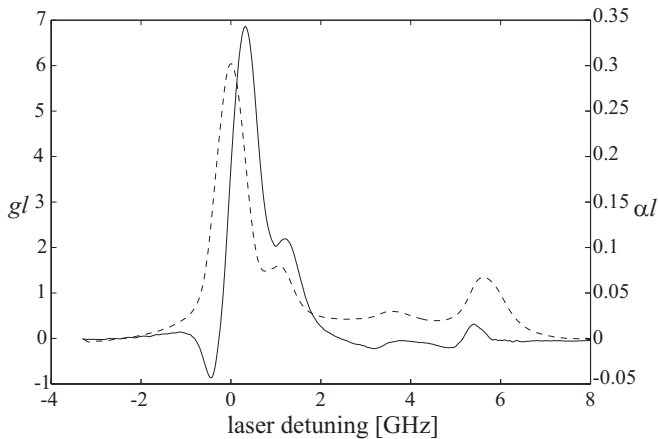


FIG. 3: Polarization self-rotation parameter gl (solid line) and absorption coefficient αl (dashed line), measured across the ^{87}Rb $D2$ line, for rubidium vapor at a temperature of 70°C . The two main features correspond to the hyperfine levels of the ^{87}Rb ground state. The hyperfine structure of the excited state is not resolved because it is narrower than both Doppler and power broadening. The “side lobes” around 1 and 4 GHz are attributed to some content of the ^{85}Rb isotope. Zero detuning corresponds to the maximum absorption point.

emerging from the cell was used as the local oscillator. To this end it was first separated from the x -polarized probe mode by means of a polarizing beam splitter and its polarization was rotated by 90° . It was then overlapped with the squeezed mode on a symmetric beam splitter. To achieve good mode matching, an auxiliary $\lambda/2$ plate placed directly after the cell was set to provide equal splitting into both polarization modes. The resulting Mach-Zehnder interferometer was carefully aligned for a maximum visibility of $V = 0.98 \pm 0.01$ corresponding to a mode matching efficiency of $V^2 \approx 0.96$. The auxiliary $\lambda/2$ plate was then removed.

A piezoelectric element was used to scan the local oscillator phase and thus the field quadrature whose fluctuations were measured. The intensities at the beam splitter outputs were measured with Si PIN photodiodes (Hamamatsu S3883 with a nominal quantum efficiency of 91%). The AC signals of the diodes were amplified with a low noise amplifier with a cutoff frequency of approximately 50 MHz and subtracted by a hybrid junction (H-9 from M/A-COM). The noise was measured with a spectrum analyzer operated in the zero span mode at a set of radio frequencies Ω_{RF} between 3 and 30 MHz with a resolution bandwidth of 1 MHz.

d. Results and discussion The squeezing homodyne measurements were performed at a finite radio-frequency Ω_{RF} , as usual, because of the high optical and electronic noise near DC. Fig. 4 shows the phase dependent noise of the x -polarization mode which contains the squeezed vacuum. It is compared to the SQL which can be measured by blocking the squeezed vacuum path. The phase

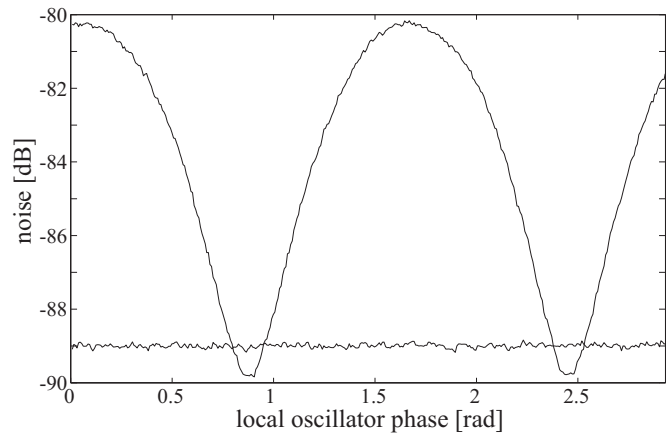


FIG. 4: Phase dependent noise and shot noise (measured by blocking the squeezed vacuum mode). Measured at $\Omega_{RF} = 5$ MHz with a laser detuning of 0.35 GHz, a resolution bandwidth of 1 MHz, a video bandwidth of 100 Hz, and a cell temperature of 70°C . A squeezing of 0.85 dB was achieved.

dependent noise minima fall below the SQL exhibiting a squeezing of (0.85 ± 0.05) dB. This corresponds to a squeezing of (1.23 ± 0.07) dB at the cell output when corrections for linear losses, inefficient photodiodes and electronic photodetector noise are made. The geometric mean noise of the squeezed mode, however, strongly exceeds the SQL so the observed ensemble is not a minimum uncertainty state. The excess noise cannot be explained by absorption alone and is presumably due to resonance fluorescence into the optical mode probed.

Fig. 5 shows the squeezing as a function of the laser detuning and the radio frequency Ω_{RF} . The variation of squeezing with the laser detuning follows approximately the self-rotation curve in Fig. 3. For small Ω_{RF} the squeezing is reduced due to extra noise from resonance fluorescence which scatters light into our vacuum mode. This extra noise was measured by misaligning the mode matching until the phase dependence vanished and maximizing the spatial overlap between the pump and probe modes in the cell by maximizing the noise. Fig. 6 shows the extra noise normalized to the vacuum noise. Its spectral width approximates the natural linewidth of $\Gamma = 6$ MHz [23], its dependence on the laser detuning is similar to the absorption line (Fig. 3). For $\Omega_{RF} \gg \Gamma$ the excess noise becomes negligible. Maximum squeezing is achieved for $\Omega_{RF} \sim 5$ MHz to 10 MHz. The reason for the squeezing to degrade with higher Ω_{RF} might be a growing phase mismatch between the pump and the probe expected in the neighborhood of an atomic resonance.

e. Summary and outlook We reported the generation of squeezed optical vacuum states in rubidium vapor with a simple setup. A squeezing of 0.85 dB was achieved which is among the best atomic vapor squeezing results accomplished. The squeezing of 6 to 8 dB predicted in [20] was not reached due to the degrading effects of self-focusing, phase mismatch and resonance

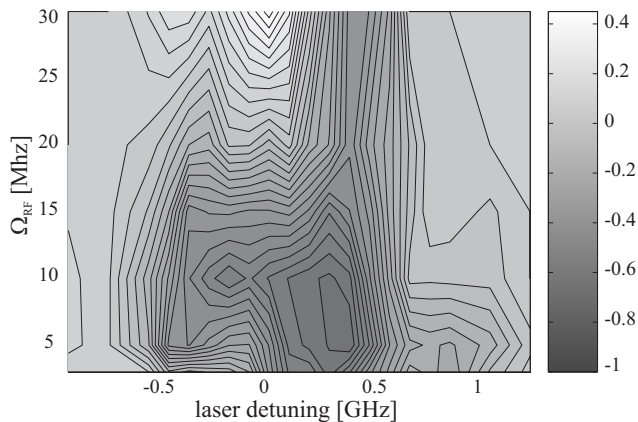


FIG. 5: Minimum quadrature noise level relative to the SQL (in dB) for a range of radio frequencies Ω_{RF} and laser detunings across one hyperfine component of the rubidium D2 line. The electronic noise has been subtracted.

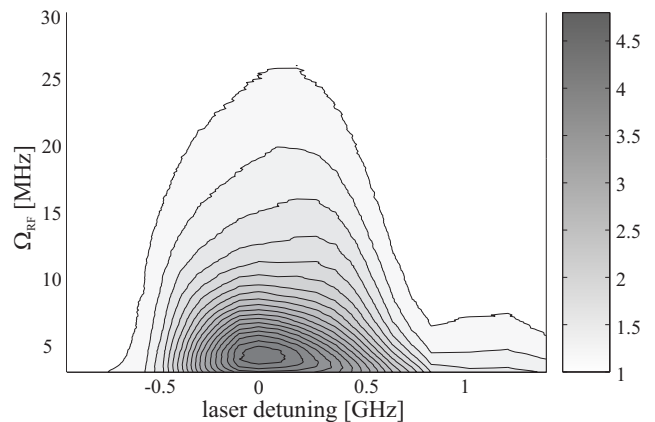


FIG. 6: Excess noise due to resonance fluorescence on a linear scale, in units of the vacuum noise for a range of radio frequencies Ω_{RF} and laser detunings. Measured by reducing the mode matching while keeping a good spatial overlap of the pump and the probe mode in the vapor cell.

fluorescence. Further theoretical investigation of these effects will help us optimize the experimental parameters. The self-rotation parameter and the associated squeezing might increase by using a cell with a moderate amount of buffer gas [24]. We are optimistic that a noticeable improvement of the squeezing is possible. By splitting the laser and directing it into several rubidium cells, numer-

ous squeezed states, which are phase locked with respect to each other, can be generated easily.

f. Acknowledgement We acknowledge helpful discussions with K. P. Marzlin, J. H. Shapiro and I. Novikova, as well as financial support from the Deutsche Forschungsgemeinschaft and the Optik-Zentrum Konstanz.

-
- [1] D. F. Walls, *Nature* **306**, 141 (1983).
 [2] R. E. Slusher, L. W. Hollberg, B. Yurke, J. C. Mertz, and J. F. Valley, *Phys. Rev. Lett.* **55**, 2409 (1985).
 [3] L.-A. Wu, H. J. Kimble, J. L. Hall, and H. Wu, *Phys. Rev. Lett.* **57**, 2520(1986).
 [4] P. Grangier, R. E. Slusher, B. Yurke, and A. LaPorta, *Phys. Rev. Lett.* **59**, 2153 (1987).
 [5] M. Xiao, L.-A. Wu, and H. J. Kimble, *Phys. Rev. Lett.* **59**, 278 (1987).
 [6] H. P. Yuen and J. H. Shapiro, *IEEE Trans. Inform. Theory* **IT25**, 179 (1979); Shapiro J. H., *Opt. Lett.* **5**, 351 (1980).
 [7] Z. Y. Ou, H. J. Kimble, and K. C. Peng, *Phys. Rev. Lett.* **68**, 3663 (1992).
 [8] A. Furusawa, J. L. Sorensen, S. L. Braunstein, C. A. Fuchs, H. J. Kimble, E. S. Polzik, *Science* **282**, 706 (1998).
 [9] S. Lloyd and S. L. Braunstein, *Phys. Rev. Lett.* **82**, 1784 (1999).
 [10] T. C. Ralph, *Phys. Rev. A* **61**, 010302 (2000).
 [11] A. Kuzmich and E. S. Polzik, *Phys. Rev. Lett.* **85**, 5639 (2000).
 [12] S. L. Braunstein, *Nature* **394**, 74 (1998).
 [13] S. Lloyd and J.-J. E. Slotine, *Phys. Rev. Lett.* **80**, 4088 (1998).
 [14] L.-M. Duan, G. Giedke, J. I. Cirac and P. Zoller, *Phys. Rev. A* **62**, 032304 (2000).
 [15] M. W. Maeda, P. Kumar, and J. H. Shapiro, *Opt. Lett.* **12**, 161 (1987).
 [16] A. Lambrecht, T. Coudreau, A. M. Steinberg, and E. Giacobino, *Europhys. Lett.* **36**, 93 (1996).
 [17] Ch. Silberhorn, P. K. Lam, O. Weiss, F. König, N. Korolkova, G. Leuchs, *Phys. Rev. Lett.* **86**, 4267 (2001).
 [18] R. M. Shelby, M. D. Levenson, S. H. Perlmutter, R. G. DeVoe, and D. F. Walls, *Phys. Rev. Lett.* **57**, 691 (1986).
 [19] M. Margalit, C. X. Yu, E. P. Ippen, and H. A. Haus, *Optics Express* **2**, 72 (1998).
 [20] A. B. Matsko, I. Novikova, and G. R. Welch, *Phys. Rev. A* **66**, 043815 (2002).
 [21] S. M. Rochester, D. S. Hsiung, D. Budker, R. Y. Chiao, D. F. Kimball, V. V. Yashchuk, *Phys. Rev. A* **63**, 043814 (2001).
 [22] W. P. Schleich, *Quantum optics in phase space* (Wiley, Berlin, 2001).
 [23] C. Cohen-Tannoudji, *Atom-photon interactions* (Wiley, Berlin, 1992); A. LaPorta, *Phys. Rev. Lett.* **59**, 2153 (1987).
 [24] I. Novikova, A. B. Matsko, and G. R. Welch, *Applied Physics Letters* **81**, 193 (2002).